Applied Physics Letters

Ion dynamics in an $E \times B$ Hall plasma accelerator

Cite as: Appl. Phys. Lett. **106**, 044102 (2015); https://doi.org/10.1063/1.4907283
Submitted: 18 December 2014 . Accepted: 16 January 2015 . Published Online: 30 January 2015

Christopher V. Young, Andrea Lucca Fabris, and Mark A. Cappelli

Ion dynamics in an $E \times B$ Hall plasma accelerator

Christopher V. Young,[a] Andrea Lucca Fabris, and Mark A. Cappelli
Stanford Plasma Physics Laboratory, 452 Escondido Mall, Bldg. 520-257, Stanford, California 94305, USA

(Received 18 December 2014; accepted 16 January 2015; published online 30 January 2015)

We show the time evolution of the ion velocity distribution function in a Hall plasma accelerator during a 20 kHz natural, quasi-periodic plasma oscillation. We apply a time-synchronized laser induced fluorescence technique at different locations along the channel midline, obtaining time- and spatially resolved ion velocity measurements. Strong velocity and density fluctuations and multiple ion populations are observed throughout the so-called "breathing mode" ionization instability, opening an experimental window into the detailed ion dynamics and physical processes at the heart of such devices. © *2015 AIP Publishing LLC*. [http://dx.doi.org/10.1063/1.4907283]

Many plasma devices operate in a quasi-steady mode with forced or naturally occurring oscillations,[1–4] and it is often desirable to capture the time-varying characteristics within one oscillation period. Parameters such as the spatially and time-dependent ion velocity distribution function (IVDF) can directly impact the performance of plasma systems and yield insight into ionization mechanisms, electric potential formation, and acceleration regions.

Hall thrusters, the well-studied $E \times B$ devices used for space propulsion applications and shown operating in Fig. 1(a), seek to ionize and accelerate propellant ions to high velocities for efficient production of thrust with high specific impulse.[5,6] These systems are rife with plasma instabilities and fluctuations, many of which elude comprehensive understanding yet are hypothesized to be critical for performance, driving electron transport across magnetic field lines and contributing to propellant ionization.[7–9] One common low frequency oscillation, often referred to as the "breathing mode," is intimately tied to the details of propellant ionization (and eventual ion acceleration) and manifests itself as a strong 10–30 kHz oscillation in the thruster discharge current. Breathing mode models suggest the presence of a propagating ionization front traversing the channel.[10,11] Experimentally, a time-averaged view of such processes[12–14] can only go so far in probing the complex physics underlying the operation of these devices. Resolving fluctuating properties at these time scales will improve our physical understanding, simulation, and design of these plasma devices.

Non-intrusive laser measurements are advantageous in that they avoid perturbing the state of the plasma. The metastable excited Xe II transition used in this work requires a continuous wave (CW) laser to resolve the narrow lineshape. Previous CW laser induced fluorescence (LIF) velocity measurements that time-synchronize with an oscillation in the plasma system have required a level of coherency only attainable by externally modulating the plasma at a known frequency. The fluorescence signal is then averaged over several cycles to achieve a reasonable signal to noise ratio. This approach has yielded interesting results when applied to measuring evolving IVDFs in Hall discharges,[15,16] pulsed argon plasmas,[17,18] and a high power impulse magnetron sputtering system.[19] Recently, MacDonald *et al.* proposed a sample-hold time-synchronized LIF scheme that allows for natural drift in the oscillation frequency without external forcing and demonstrated the technique on 60 Hz oscillations in a xenon discharge lamp[20] and 3 kHz oscillations in a cusped plasma accelerator.[21]

In this letter, we apply a time-synchronized sample-hold LIF method of measuring time-varying xenon ion velocities to an $E \times B$ Hall plasma accelerator with quasi-coherent 20 kHz natural oscillations. We extend the method to higher frequencies than previously reported[21] and demonstrate its utility on a new plasma device—one of many naturally oscillating or driven plasma systems whose ion dynamics could be interrogated in fine detail using this approach. By examining the time histories of the acquired LIF lineshapes at four axial locations along the channel midline, we show how the near-field ion velocity and probed metastable state density change throughout one Hall thruster breathing mode cycle. The emergence of a low velocity ion population in the plume, apparent during only part of the oscillation, could have greater ramifications for designing electric propulsion systems with regards to spacecraft charging concerns and ground-based testing effects.

The Z-70 laboratory Hall thruster used in this work (described further in Refs. 22 and 23) derives its designation from the outer diameter of the discharge channel: 72 mm. The annular anode/propellant distribution system sits at the base of the channel, 23 mm from the exit plane, with an inner diameter of 42 mm. The thruster consumes 1.97 mg/s of xenon and operates at an average power of 357 W (with 300 V of applied anode potential) in the strong 20 kHz oscillatory mode shown in Fig. 1(b). An FFT of the discharge current signal shows that the fundamental frequency and its harmonics naturally drift about the average values, which the time-synchronized LIF method must tolerate. The thruster runs with an external IonTech barium oxide hollow cathode (with a 150 μg/s argon propellant feed) located 2 cm downstream and 7 cm radially outwards from the thruster main axis, pointing at about 45°. 1.19 A of current is driven through the magnet coils, producing a primarily radial magnetic field of ~100 G at the intersection of the channel midline and the exit plane.

We give a brief description of the time-synchronized LIF system here; further detail may be found in Ref. 23.

[a]Electronic mail: cvyoung@stanford.edu

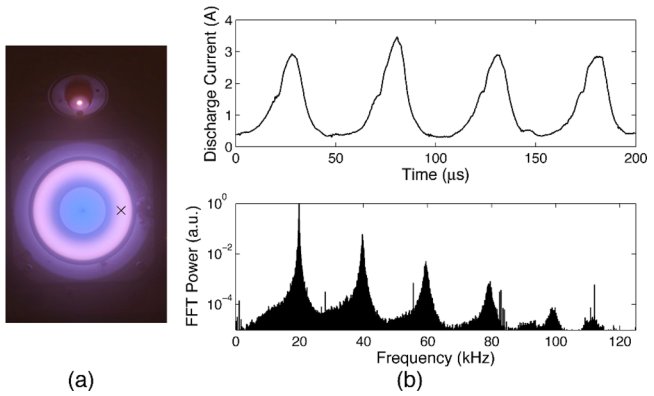

FIG. 1. (a) Z-70 Hall thruster (with external cathode above) running on krypton in the Stanford Plasma Physics Laboratory. The "×" indicates the measurement axis. (b) Discharge current and FFT (log scale) showing the strong 20 kHz breathing mode oscillation and its harmonics.

The laser and vacuum systems are identical to those used previously in time-averaged LIF velocity experiments.[24] A cryogenic pumping system achieves a base pressure of 1×10^{-6} Torr (uncorrected for xenon) and maintains a background pressure of 5×10^{-5} Torr during thruster operation. We use ~40 mW of amplified, tunable diode laser power to pump the $5d[4]_{7/2} - 6p[3]_{5/2}$ Xe II transition at 834.724 nm (air). Resulting fluorescence photons emitted at 541.915 nm (air) during relaxation to the $6s[2]_{3/2}$ state are collected through two 100 mm diameter, 200 mm focal length lenses, two 10 nm bandpass filters centered at 540 nm and 543.5 nm, and a photomultiplier tube. A small iris yields ~1 mm^3 spatial resolution.

Beam diagnostics accurately reconstruct the laser wavelength scan. A stationary frequency reference is obtained using the optogalvanic effect with the $6s'[1/2]_1 - 6p'[3/2]_2$ Xe I transition at 834.682 nm (air) in a xenon hollow cathode lamp. This line is separated 18.1 GHz from the stationary Xe II line used for ion velocimetry. A Fabry-Perot interferometer with 1.5 GHz FSR and a finesse of 200 provides fixed frequency markers during the scan. The laser is optically chopped at 2.5 kHz, enabling a lock-in amplifier to extract the fluorescence signal from the bright plasma background emission using phase-sensitive homodyne detection. When the lock-in receives the PMT signal directly, we obtain a time-averaged fluorescence excitation spectrum[24] with a peak intensity that has been Doppler shifted an amount $\Delta\nu$ away from the nominal value ν_0 (359 THz = 834 nm) expected for the transition. The most probable axial xenon ion velocity component along the laser beam direction is then given by $v_{Xe} = \Delta\nu/c\,\nu_0$.

Time synchronization between the fluorescence signal and thruster discharge current is achieved with a comparator chip that triggers when the current crosses an adjustable threshold value, indicating the start of a new cycle. This technique allows for natural frequency drift in the current, since the comparator always identifies the next cycle independently from the previous one. A pulse generator produces a short measurement gate with a tunable delay time Δt from the "zero phase" time origin identified by the comparator. Once per current cycle, fluorescence signal is averaged within each measurement gate and held until the following gate, at which point the held value is updated with the new average. This effectively excludes all fluorescence signal from the lock-in amplifier that does not originate during the target phase of the discharge current. Since the exciting laser beam is still optically chopped, the fluorescence peak associated with delay time Δt is extracted by the lock-in using phase-sensitive detection as in the standard time-averaged scheme.

We apply the time-synchronized diagnostic at four spatial locations along the channel midline in 5 mm increments from the exit plane ($z = 0$ mm) to $z = 15$ mm downstream (see Fig. 1(a)). This region contains the greatest axial acceleration of xenon ions in the thruster. LIF traces are taken every 5 μs along the discharge current oscillation with a 2 μs measurement gate.

The most probable axial ion velocities obtained as a function of time, synchronized with the 20 kHz discharge current oscillation, are shown in Fig. 2(a). The complete ion energy distribution function may be deconvolved from the LIF lineshape given sufficient information regarding spectroscopic constants and discharge parameters, although previous work with this Xe II line in Hall discharges suggests that deconvolution may not be necessary to resolve the IVDF.[14] The most probable ion velocity is recovered simply from the location of the Doppler-shifted LIF signal peak. The 40 mW of laser excitation remains close to the linear fluorescence regime and mild saturation, if any, in the LIF signal does not alter its peak location.[13]

The results of Fig. 2(a) show strong fluctuations in the axial xenon ion velocities over one discharge current cycle, throughout the plume. At all locations studied, the velocity is

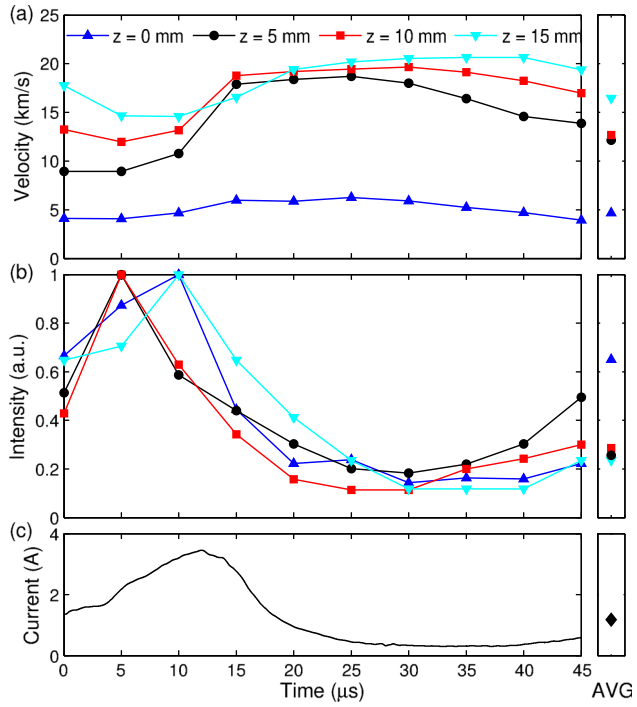

FIG. 2. (a) Time histories of the most probable axial xenon ion velocities measured in the thruster plume showing strong ion acceleration downstream of the exit plane. (b) Time dependence of the LIF signal peak intensity normalized to the maximum value at each spatial point. (c) Discharge current profile for orienting the time axis. The boxes at right show the corresponding values obtained from a time-averaged measurement.

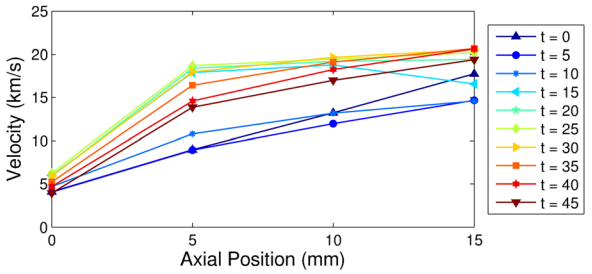

FIG. 3. Most probable axial ion velocities as a function of spatial location, showing the changing shape of the plume's acceleration field over the discharge current cycle. The time unit is μs.

observed to be ~50% of the maximum value during the ramp up in discharge current, after which the velocities are quickly accelerated to near the maximum value as the current ramps down. The velocities stay high until the start of the next cycle, at which point they drop again to ~50%. Significant ion acceleration occurs in the first 5 mm after the exit plane. Such velocity variations are likely due to transient ionization and electric potential structures also fluctuating on the order of the discharge current cycle, as discussed further below.

Fig. 2(b) reports how the peak LIF signal intensity (normalized to the maximum observed at each spatial location) varies throughout the oscillation cycle. Signal intensity is proportional to the local probed excited state ion density (which does not necessarily indicate the ground state ion density, but is correlated), and the observed trends can be understood in accordance with standard models of the Hall thruster breathing mode.[10,11] An ionization front propagates towards the exit plane, increasing in strength as it approaches the region of maximum magnetic field. As the ionization rate increases along with elevated discharge temperature, there is a corresponding increase in discharge current from primary and secondary electrons reaching the anode. This is seen in Fig. 2(b) as the maximum LIF signal intensities peak near the end of the ramp up in discharge current. Then, as the ions are accelerated away by the electric field and the ionization front turns back towards the anode, the local ion density necessarily decreases. This is also observed. The discharge current falls as the ionization front moves away from the region of peak magnetic field, with a corresponding decreased ionization rate. This state is apparent in the data as a period of relatively constant ion velocity, low LIF signal intensity, and low discharge current.

The measured velocity data also give insight into the time-varying spatial distribution of the acceleration field in the near field plume region of the thruster. Fig. 3 plots the most probable axial velocities as a function of space at different time points along the discharge current cycle. Three distinct regions may be identified. At early times during the discharge current ramp up, there is roughly constant acceleration over the 15 mm domain studied. Then, after the discharge current peak, there is a sharp acceleration over the first 5 mm with little subsequent change in velocity downstream. At $t = 15\,\mu$s, the most probable axial velocity at $z = 15$ mm is even observed *slower* than that upstream at $z = 5$ and 10 mm. Here, a high velocity ion population has been produced upstream and will soon overtake a slower population left over from the previous cycle. This process has been observed in 2D Hall thruster simulations as well (see, for example, Fig. 8 of Ref. 25). Lastly, during the discharge current trough, the spatial velocity profile progressively becomes more linear as before and the cycle repeats. This data suggest that the near-field accelerating potential structure in the discharge is also fluctuating on the time scale of the breathing mode oscillation.

Finally, additional information may be obtained by examining the full suite of LIF lineshapes collected, not just the peak locations. These data are presented as contour maps in Fig. 4, one for each spatial location in the plume. Each laser scan (a vertical slice spanning frequency space at a given time and location) is normalized by the total intensity

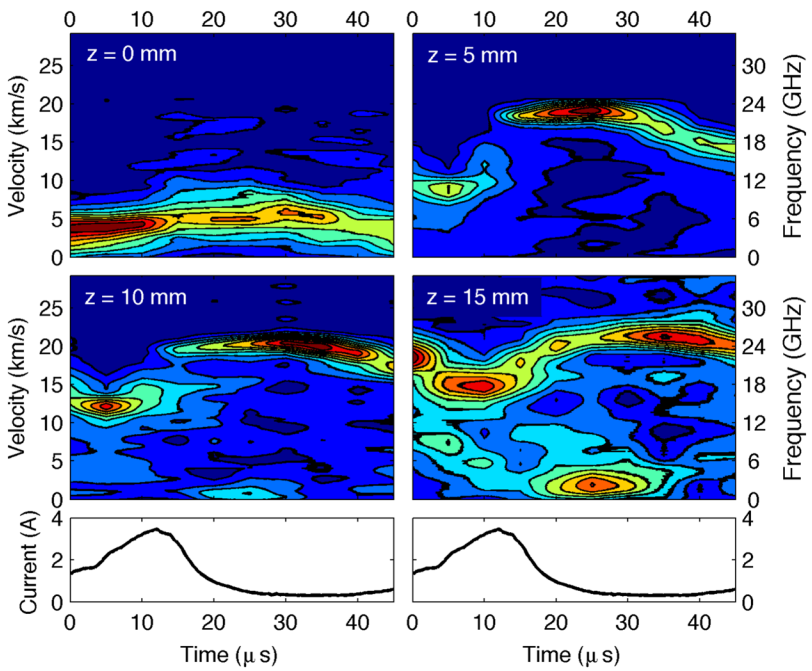

FIG. 4. Contour maps of measured LIF lineshapes obtained at 5 μs intervals in 5 mm steps along the channel centerline, downstream of the exit plane ($z = 0$). A single laser scan (over frequency space) constitutes a vertical strip at a given time delay. Each trace is normalized by the total intensity of the scan (sum of all values collected) to show structure despite the significant reduction in signal intensity at later delay times (see Fig. 2(b)). The discharge current trace at bottom orients the time axis. Note the appearance of a slow velocity ion population emerging 15 mm into the plume, which may be due to charge exchange collisions with neutral xenon atoms or finite background pressure chamber effects.

of the scan (sum of all values collected) so the features are not obscured by the decreasing signal intensity (see Fig. 2(b)). This normalization also facilitates comparison between scans of the relative fluorescence peak widths and fraction of total intensity occurring in the main peak feature. By connecting the areas of peak fluorescence over time, one obtains the most probable velocity curves shown in Fig. 2(a). Recall that data are only taken at 5 μs increments, producing visual gaps in the contours between data points.

The width of the fluorescence feature is related to the spread in excited state ion velocities present at that location in time and space. At the exit plane where velocities are slower, there exists greater variation about the peak value. This could be due to an upstream ionization region of finite thickness producing ions that then fall through differing amounts of a relatively shallow potential drop. By 5 and 10 mm downstream, this spread persists during the slower velocity region at early times; however, the highest velocity ion populations that form after the discharge current peak exhibit a narrower distribution. By $z = 15$ mm, the increased background noise makes this determination more difficult.

An interesting feature arises between $t = 20$ and 30 μs, 15 mm into the plume: the formation of a low ion velocity population. Hints of its development may be seen at $z = 10$ mm, at a level barely above the noise. For a short period in time, new ions are generated out in the plume—not in the typical ionization zones near the channel exit—and thus experience only a fraction of the accelerating potential drop traversed by their high velocity counterparts. This feature has been observed before in time-averaged velocity measurements in the near-field of a 200 W Hall thruster,[26] and is reproduced in our time-averaged LIF traces (not shown). The time-resolved data shows how, contrary to what might be expected from the time-averaged view, this slow population only persists for a portion of the oscillation cycle. The presence of this low velocity population may be explained either by charge exchange collisions with neutrals or by finite background chamber pressure effects (ionization of neutrals not removed by the cryogenic vacuum pumps). Future studies will examine the time-synchronized neutral velocity distribution at this location for evidence of a corresponding high velocity neutral population during this time interval, symptomatic of charge exchange collisions.

The time-varying ion velocity distribution in Hall thruster plumes is the product of the complicated phase space histories of particles generated in time- and spatially-dependent ionization zones, accelerated by time- and spatially-dependent electric fields. Time-synchronized measurements at four spatial locations only scratch the surface of this complex dynamic flow field, but interesting physics that would otherwise be obscured with a time-averaged measurement are already apparent.

In summary, we have utilized xenon ion laser induced fluorescence velocimetry to measure axial xenon ion velocities in an un-driven Hall plasma accelerator, synchronized in time with a 20 kHz breathing mode oscillation. Plume measurements show strong fluctuations in the xenon ion axial velocities and local excited state densities over the 20 kHz cycle. Strong ion acceleration occurs near the peak in the discharge current, and ion density falls off dramatically as accelerated ions depart the thruster. The near field spatial acceleration field oscillates in time between a near constant value over the full 15 mm, and a jump in the first 5 mm with little subsequent acceleration. A low velocity ion population arises 15 mm into the plume during the falling discharge current ramp, which could be due to charge exchange collisions or background chamber pressure effects. Future studies will explore these phenomena and use hybrid simulations[27] to further our understanding of the basic physics driving time-dependent ionization, acceleration, and electron transport in these devices.

The authors thank N. Gascon for helpful discussions. This work was sponsored by the U.S. Air Force Office of Scientific Research with Dr. M. Birkan as Program Manager. C.Y. acknowledges support from the DOE NSSA Stewardship Science Graduate Fellowship under contract DE-FC52-08NA28752 and the Stanford Graduate Fellowship.

[1]J.-P. Boeuf and B. Chaudhury, Phys. Rev. Lett. **111**, 155005 (2013).
[2]A. Smolyakov, W. Frias, I. Kaganovich, and Y. Raitses, Phys. Rev. Lett. **111**, 115002 (2013).
[3]C. Schröder, O. Grulke, T. Klinger, and V. Naulin, Phys. Plasmas **12**, 042103 (2005).
[4]E. Martines, R. Cavazzana, G. Serianni, M. Spolaore, L. Tramontin, M. Zuin, and V. Antoni, Phys. Plasmas **8**, 3042 (2001).
[5]V. Kim, J. Propul. Power **14**, 736 (1998).
[6]M. A. Cappelli, Phys. Today **62**(4), 76 (2009).
[7]N. B. Meezan, W. A. Hargus, and M. A. Cappelli, Phys. Rev. E **63**, 026410 (2001).
[8]N. B. Meezan and M. A. Cappelli, Phys. Rev. E **66**, 036401 (2002).
[9]C. A. Thomas, N. Gascon, and M. A. Cappelli, Phys. Rev. E **74**, 056402 (2006).
[10]S. Barral and E. Ahedo, Phys. Rev. E **79**, 046401 (2009).
[11]J.-P. Boeuf and L. Garrigues, J. Appl. Phys. **84**, 3541 (1998).
[12]R. Cedolin, W. Hargus, Jr., P. Storm, R. Hanson, and M. Cappelli, Appl. Phys. B **65**, 459 (1997).
[13]W. Hargus, Jr. and M. Cappelli, Appl. Phys. B **72**, 961 (2001).
[14]D. Gawron, S. Mazouffre, N. Sadeghi, and A. Héron, Plasma Sources Sci. Technol. **17**, 025001 (2008).
[15]S. Mazouffre and G. Bourgeois, Plasma Sources Sci. Technol. **19**, 065018 (2010).
[16]J. Vaudolon, L. Balika, and S. Mazouffre, Rev. Sci. Instrum. **84**, 073512 (2013).
[17]C. Biloiu, X. Sun, E. Choueiri, F. Doss, E. Scime, J. Heard, R. Spektor, and D. Ventura, Plasma Sources Sci. Technol. **14**, 766 (2005).
[18]I. A. Biloiu, X. Sun, and E. E. Scime, Rev. Sci. Instrum. **77**, 10F301 (2006).
[19]M. Desecures, L. de Poucques, T. Easwarakhanthan, and J. Bougdira, Appl. Phys. Lett. **105**, 181120 (2014).
[20]N. MacDonald, M. Cappelli, and W. Hargus, Jr., Rev. Sci. Instrum. **83**, 113506 (2012).
[21]N. MacDonald, M. Cappelli, and W. Hargus, Jr., J. Phys. D: Appl. Phys. **47**, 115204 (2014).
[22]A. W. Smith, "Field structure and electron transport in the near-field of coaxial Hall thrusters," Ph.D. dissertation (Stanford University, 2010).
[23]See supplementary material at http://dx.doi.org/10.1063/1.4907283 for a schematic of the Z-70 Hall thruster geometry and further details regarding the time-synchronized LIF system. (2015).
[24]A. L. Fabris, C. V. Young, M. Manente, D. Pavarin, and M. A. Cappelli, IEEE Trans. Plasma Sci. **43**, 54 (2015).
[25]J. Bareilles, G. Hagelaar, L. Garrigues, C. Boniface, J. Boeuf, and N. Gascon, Phys. Plasmas **11**, 3035 (2004).
[26]A. Lejeune, G. Bourgeois, and S. Mazouffre, Phys. Plasmas **19**, 073501 (2012).
[27]M. K. Scharfe, N. Gascon, M. A. Cappelli, and E. Fernandez, Phys. Plasmas **13**, 083505 (2006).